A new computational method for cable theory problems

Bulin J. Cao and L. F. Abbott

Physics Department and Center for Complex Systems, Brandeis University, Waltham, MA 02254 USA

ABSTRACT   We discuss a new computational procedure for solving the linear cable equation on a tree of arbitrary geometry. The method is based on a simple set of diagrammatic rules implemented using an efficient computer algorithm. Unlike most other methods, this technique is particularly useful for determining the short-time behavior of the membrane potential. Examples are presented and the convergence and accuracy of the method are discussed.

1. INTRODUCTION

Cable theory is the primary tool used to relate the geometric form of a neuron to its electrical function (1-3). The basic problem of cable theory is to compute the membrane potential everywhere on a complex neuron as a function of the external and synaptic currents entering the cell. Much work has been done for neurons with restricted dendritic structures (4-7) satisfying, for example, Rall's 3/2 power rule (8). In addition, several powerful and practical techniques have been developed to solve the cable equation for neurons with dendritic trees of arbitrary geometry (9-17). Because dendritic trees are typically so elaborate, it is essential that any general computational method be relatively simple to implement, even for complex trees, and easy to code for computer calculations, which are essential for all but the simplest structures. Particularly noteworthy among the various methods available are diagrammatic rules for computing the Laplace transform of the cable potential developed by Butz and Cowan (9) and, perhaps the most widely used method, compartmentalization (13, 14) with efficient computer implementation (15). On the basis of a path integral approach, a new method for solving cable theory problems has recently been developed by E. Farhi, S. Gutmann, and one of us (16, 17). The method is based on a remarkably simple set of diagrammatic rules which, in contrast to virtually all other general methods, are ideally suited for investigating the short-time behavior of the membrane potential on a dendritic tree. These rules have been derived elsewhere (16, 17). Here we will show how the new diagrammatic approach for solving cable problems can be efficiently implemented on a computer and will exhibit the results for several sample structures. We will pay particular attention to the convergence and accuracy of the method.

Of all the methods for analyzing the potential on a complex dendritic structure, compartmentalization is the most powerful and general. This is because it is the only method that allows a full treatment of the voltage-dependent membrane conductances and time-dependent synaptic conductances found in real neurons. Non-compartmental cable theory methods, including the one

used here, require us to assume that over the voltage range being considered, the membrane conductance is approximately constant (although see (18)). In addition, the non-compartmental methods typically treat synapses as sites of current injection, ignoring the accompanying synaptic conductance changes (although see (8, 19-23)). This is only valid if the synaptic contribution to the total membrane conductance is small. The fact that the compartmental approach does not require these assumptions makes it an attractive and powerful alternative. The biggest disadvantage of the compartmental method is that it does not provide a continuous description of the potential as a function of position but rather a discrete approximation to it. Consider the potential that results from a localized spike of current injected into a dendritic structure. Shortly after the spike is injected, the potential on the tree varies rapidly as a function of position so the compartmental approximation is poor and a continuous description is desirable. As time passes, the potential becomes more uniform and the validity of the compartmental approximation increases. To complement the compartmental method, we need an approach that provides a continuous description and is accurate at short times when the compartmental technique breaks down. This is precisely what the method presented here provides. It is ideally suited for computing rise and response times and other short-time phenomena.

When we use a voltage-independent approximation for the membrane conductance, the electrotonic characteristics of a dendritic tree can be parameterized by three quantities: the resistivity of the intracellular fluid r, the membrane capacitance per unit area C, and the membrane conductance per unit area which we denote by $1/R$. We will assume that these three parameters are the same on all branches of the tree (the case of a spatially varying membrane conductivity is considered in (16) but this case is much more difficult to compute). The radius of a given branch of the tree will be denoted by a_{seg} where seg labels a particular segment of the tree. (All segments are taken to be cylinders, a tapering cable can be treated as a sequence of cylindrical segments joined at non-branching nodes.) The formulas of cable theory are simpler if we measure all distances along segment seg in units of the electrotonic length constant $(Ra_{seg}/2r)^{1/2}$
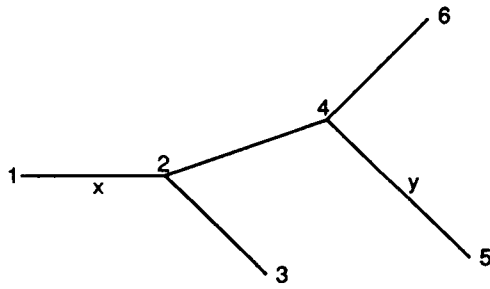
FIGURE 1 A dendritic tree with labeled nodes and terminals. The point marked x indicates where the potential is measured and y indicates the site of current injection. The points marked 2 and 4 are nodes and 1, 3, 5, and 6 are terminals.

and all times in units of the membrane time constant RC and we will do this throughout. The geometric structure of the trees we consider is completely general. A tree is made of a number of segments that meet at nodes and end at terminals. For example, in Fig. 1, the points marked 2 and 4 are nodes and 1, 3, 5, and 6 are terminals. An arbitrary number of segments can meet at a node and there is no restriction on their radii or on their lengths.

Let $V(x, t)$ be the membrane potential at time t measured at point x. (Since dendrites have multiple branches, we really should identify the particular segment along which the point x is located, by using a subscript, for example (see (16, 17)), but we will ignore this complication, except where it is unavoidable.) We define the potential V so that $V = 0$ is the resting potential of the neuron. V satisfies the cable equation

$$\frac{\partial V}{\partial t} = \frac{\partial^2 V}{\partial x^2} - V + I(x, t) \tag{1.1}$$

where $I(x, t)$ is the current (in appropriate units) being injected at the point x at time t. In addition to solving this equation, the potential V must satisfy boundary conditions at all of the nodes and terminals of the tree. At a node, V must be continuous as we cross from one segment to another and current must be conserved. At a terminal, various different boundary conditions can be imposed. We will require that no current flows through a terminal, the so-called "sealed end" condition. A trivial modification of the diagrammatic rules allows the "killed end" condition to be treated as well (16, 17) but we will not consider this case here.

The potential V depends on the current I being injected into the tree and it also depends on the geometric and electrotonic structure of the tree. These two dependencies can be separated by expressing the potential V in terms of a Green's function,

$$V(x, t) = \int dy \left[G(x, y, t)e^{-t}V(y, 0) \right.$$

$$\left. + \int ds G(x, y, t - s)e^{s-t}I(y, s) \right]. \tag{1.2}$$

We include the exponential factors in Eq. 1.2 to simplify the definition of the Green's function $G(x, y, t)$. The advantage of using the Green's function is that it depends only on the structure of the tree and not on the injected current. Therefore, it only has to be computed once for a given dendritic structure. If the tree is initially at its resting potential, $V(x, 0) = 0$, the first term in Equation 1.2 can be ignored. In this case, $G(x, y, t)e^{-t}$ is the potential measured at time t at the point x in response to an instantaneous spike of current of unit integral strength (a delta function) injected at the point y at time zero. This provides a physical interpretation of the meaning of the Green's function. Once G is known, Eq. 1.2 allows the potential to be constructed for any initial condition and distribution of currents.

2. THE DIAGRAMMATIC RULES

The computer program we have developed and results we will present are based on a simple diagrammatic algorithm for computing the Green's function for any dendritic tree. The basic idea is to express the Green's function as a sum over "trips" (16, 17). Each trip represents one term in a series giving the exact Green's function. Specifically, for any dendritic structure

$$G(x, y, t) = \sum_{\text{trips}} A_{\text{trip}}G_0(L_{\text{trip}}, t) \tag{2.1}$$

where the sum is over all possible trips constructed using the rules given below, L_{trip} is the length of the trip being summed and

$$G_0(L_{\text{trip}}, t) = \left(\frac{1}{4\pi t}\right)^{1/2} \exp\left[-\frac{L_{\text{trip}}^2}{4t}\right]. \tag{2.2}$$

Also given below are the rules for determining the coefficients A_{trip} which depend on the particular trip being summed.

A trip is a path along the tree that starts at the point x (the point where the potential is being measured) and ends at the point y (the point where the current is being injected). Trips are constructed in accordance with the following rules:

- A trip may start out from x by traveling in either direction, but it may subsequently change direction only at a node or a terminal. A trip may pass through the points x and y an arbitrary number of times but must begin at x and end at y.
- When a trip arrives at a node, it may pass through the node to any other segment radiating from the node or it may reflect off the node back along the same segment on which it entered.
- When it reaches a terminal, a trip always reflects back, reversing its direction.

Every unique trip generates a term in the sum (2.1) for the Green's function. L_{trip} is the total length (in units of the electrotonic length constants) of the trip obtained by summing all the steps taken along the course of the trip.
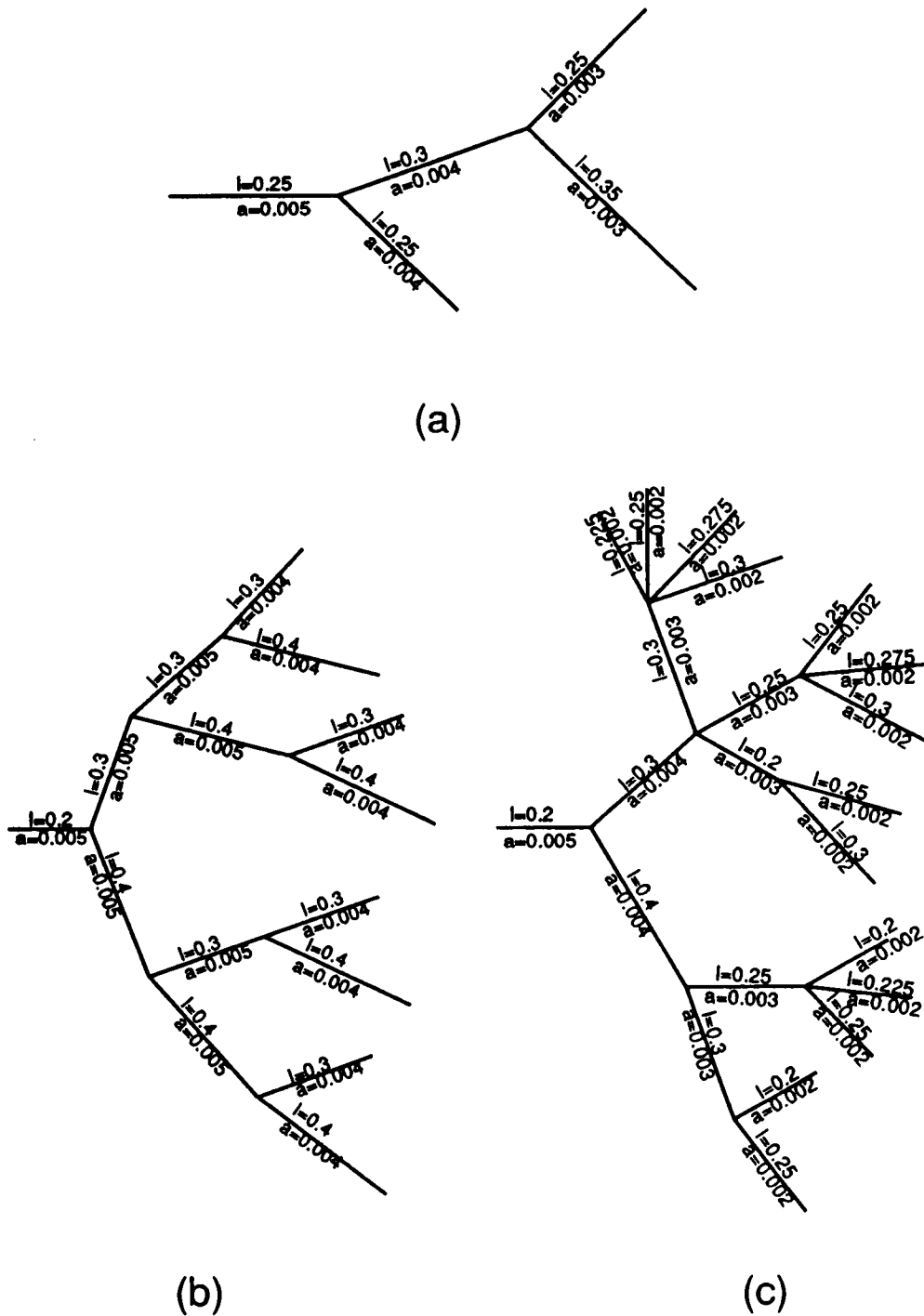
(a)

(b)

(c)

FIGURE 2   The sample trees used for subsequent figures. All measurements are in electrotonic units. The radii of the branches are labeled by a and their lengths by l.

For any given trip, the coefficient A_{trip} is computed from the following rules:

- Initially when the trip starts out from the point x, $A = 1$.
- As the trip progresses from x to y, A is multiplied by a factor every time the trip passes through or reflects off a node. Let S be the sum of the three-halves

power of the radii of each of the segments radiating from the node in question,

$$S = \sum_{\text{seg on node}} a_{\text{seg}}^{3/2} \qquad (2.3)$$

and let a_{out} be the radius of the segment along which the trip leaves the node. If the trip passes through the node, A is multiplied by the factor

$$\frac{2a_{out}^{3/2}}{S} \qquad (2.4)$$

while if the trip reflects off the node, A is multiplied by

$$\frac{2a_{out}^{3/2}}{S} - 1. \qquad (2.5)$$

- When the trip reflects off a terminal, A remains unchanged.

(If a killed-end boundary condition is used instead, the last rule is changed so that A changes sign when the trip reflects off a terminal.)

The proof that the above rules produce the correct Green's function solving the cable problem is given in (16, 17). The rules given above require that the trips be generated starting at the point x and ending at the point y. Sometimes it is more convenient to start the trips at y and travel to x instead. If reversed trips going from y to x are used, the result of summing the trips will be $G(y, x, t)$. However, the simple identity

$$G(x, y, t) = \left(\frac{a_y}{a_x}\right)^{3/2} G(y, x, t) \qquad (2.6)$$

allows the properly ordered Green's function to be computed using reversed trips. In this formula a_x is the radius of the segment on which x is located and a_y the radius where y is located.

3. COMPUTER IMPLEMENTATION

The sum over trips (2.1) that determines the Green's function is, in general, an infinite sum. For any practical computational scheme, this sum must be truncated. Since the individual terms involve the factor $\exp(-L_{trip}^2/4t)$ appearing in Eq. (2.2), long trips are exponentially suppressed and are especially insignificant when t is small. This is why the method is particularly accurate in the short-time limit. We truncate the sum over trips by introducing a length cutoff and ignoring all trips longer than this cutoff. We will study the effect that this truncation has on the accuracy of the results.

Since the trips we have to sum to determine the Green's function and solve the cable problem are generated by simple rules, the diagrammatic method can be implementation by an efficient, recursive computer algorithm. We have constructed such a program (24) that runs on a UNIX workstation (DEC 5000). The program is written in C and, for the examples shown below, takes anywhere from a fraction of a second (for hundreds of trips) to about a minute (for tens of thousands of trips) to compute the sum over trips.

The algorithm we use starts by dividing the trips into four classes. The classes are defined according to the nature of the first and last steps of the trip. We will use the simple tree shown in Fig. 1 to illustrate how the classes of trips are defined. Trips leaving the point x in Fig. 1 may travel first to node 2 or may start out in the opposite direction traveling first to terminal 1. Similarly when the trips finally end up at the point y they may arrive from node 4 or from terminal 5. The four different combinations of the possibilities enumerated define the four classes of trips: 1) trips that start $x \rightarrow 2$ and end $4 \rightarrow y$, 2) trips that start $x \rightarrow 2$ and end $5 \rightarrow y$, 3) trips that start $x \rightarrow 1$ and end $4 \rightarrow y$, and 4) trips that start $x \rightarrow 1$ and end $5 \rightarrow y$.

The program starts by constructing the shortest trip in each class. Since a trip can only change direction at a node or terminal, its path can be specified by listing the sequence of nodes and terminals contacted along the journey from x to y. For the tree in Fig. 1, the shortest trips in each of the four classes are: $x \rightarrow 2 \rightarrow 4 \rightarrow y$, $x \rightarrow 1 \rightarrow 2 \rightarrow 4 \rightarrow y$, $x \rightarrow 2 \rightarrow 4 \rightarrow 5 \rightarrow y$ and $x \rightarrow 1 \rightarrow 2 \rightarrow 4 \rightarrow 5 \rightarrow y$. The sum of these four trips with appropriate factors gives the lowest order approximation to the Green's function. (Actually, the single trip $x \rightarrow 2 \rightarrow 4 \rightarrow y$ gives the lowest order approximation (16) but we will keep all four terms.) At every stage in the computation of the Green's function, we will continue to divide trips into these four classes. Although the strict segregation of trips into classes may seem artificial, it turns out that keeping members of each class at every stage of the calculation dramatically improves its accuracy.

To calculate the Green's function accurately, we must sum over more than just the shortest trip in each class. However, to keep the number of terms to be summed finite we must impose a length cutoff on the trips. This is done by comparing the length of a trip in any given class to the length of the shortest trip in that class. If this difference is less than a predefined cutoff length the trip is summed, if not it is ignored. The sum of the four shortest trips discussed above corresponds to a length cutoff of zero.

If the length cutoff is greater than zero, we must generate other trips besides the shortest one in each class. We do this by adding excursion from the nodes and terminals that a trip contacts along its path from x to y. For example, consider the trip $x \rightarrow 2 \rightarrow 4 \rightarrow y$ for the tree of Fig. 1. To generate a longer trip within this same class, we add to this trip all possible excursions from the two nodes that it passes through, 2 and 4. An excursion is a trip that starts and ends at the same point. We do this sequentially by adding two-step excursions, one at a time. A two-step excursion is a trip that leaves a certain node or terminal, reflects off the first other node or terminal that it encounters, and then returns to where it started. For the trip $x \rightarrow 2 \rightarrow 4 \rightarrow y$, we can add the two-step excursion $2 \rightarrow 1 \rightarrow 2$ giving the longer trip $x \rightarrow 2 \rightarrow 1 \rightarrow 2 \rightarrow 4 \rightarrow y$. Similarly, we can add the excursions $2 \rightarrow 3 \rightarrow 2$ and $2 \rightarrow 4 \rightarrow 2$ producing the trips $x \rightarrow 2 \rightarrow 3 \rightarrow 2 \rightarrow 4 \rightarrow y$ and $x \rightarrow 2 \rightarrow 4 \rightarrow 2 \rightarrow 4 \rightarrow y$. In addition, we can add the excursions $4 \rightarrow 2 \rightarrow 4$, $4 \rightarrow 5 \rightarrow$
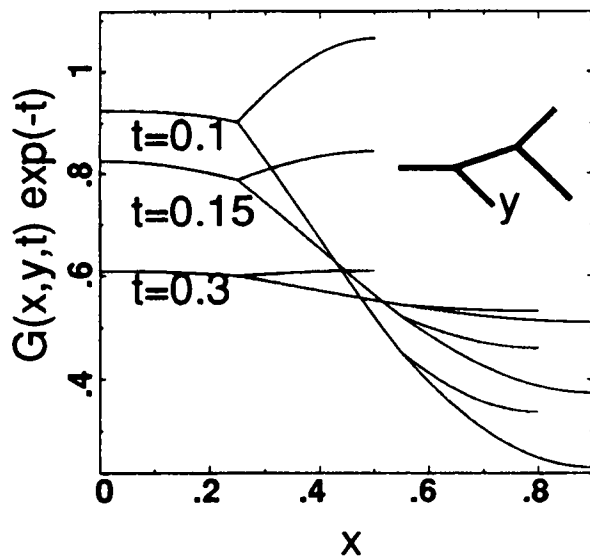
(a)
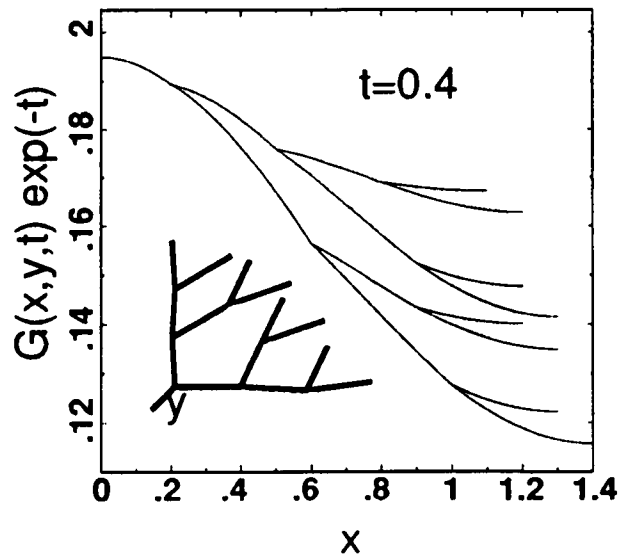
(b)
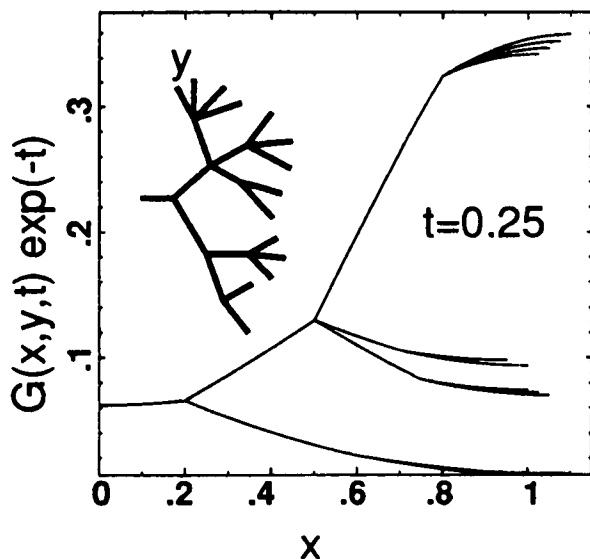
(c)

FIGURE 3   The potentials produced by a delta-function spike of current injected at the point marked y in the inserted diagrams and measured at x at the times indicated. The current injection site is near the end of the segment where y is indicated. Panels a, b, and c correspond to the trees of Fig. 2 a, b, and c respectively. The coordinate x measures electrotonic distance from the base of the tree and the different branches appear as multiple lines on the plots. Fig. 3 a shows three different times, while b and c show the potential at the single time indicated.

4 and $4 \to 6 \to 4$ to the node 4 producing the trips $x \to 2 \to 4 \to 2 \to 4 \to y$, $x \to 2 \to 4 \to 5 \to 4 \to y$ and $x \to 2 \to 4 \to 6 \to 4 \to y$. This illustrates one step in the iterative procedure we use to generate all trips. It also

points out a potential problem. In this construction the trip $x \to 2 \to 4 \to 2 \to 4 \to y$ has been generated twice, once by adding the excursion $2 \to 4 \to 2$ to node 2 and once by adding $4 \to 2 \to 4$ to node 4. Each trip occurs
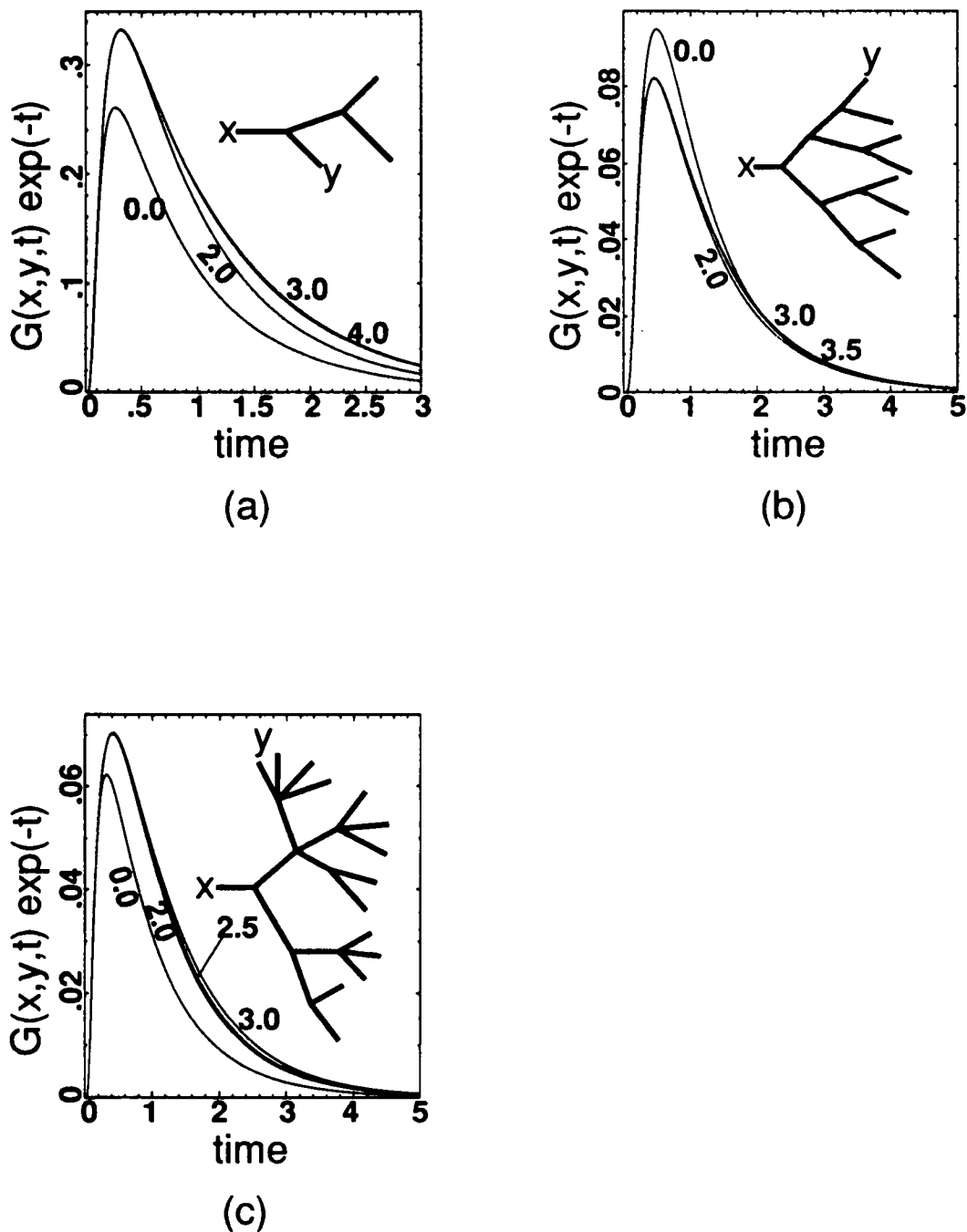
FIGURE 4 The potential produced by a delta-function spike of current injected at the point marked y and measured at the point marked x in the inserted diagrams, plotted as a function of time. Panels a, b, and c correspond to the trees of Fig. 2 a, b, and c, respectively. The different curves correspond to the different length cutoffs indicated. Note that even the curve for zero-length cutoff is a fairly good approximation, and that for length cutoffs greater than 3 the curves converge.

only once in the sum over trips so such double counting must be avoided by eliminating any trips generated more than once.

The trips generated above can be lengthened still further by adding all possible two-step excursions from their nodes and terminals. For example, the trip $x \to 2 \to 4 \to 6 \to 4 \to y$ can be lengthened by adding two-step excursion from nodes 2 and 4 and terminal 6. Note that an

excursion starting at node 4, such as $4 \to 5 \to 4$, can be added to this trip in two ways, either by adding it the first time node 4 appears in the sequence giving the trip $x \to 2 \to 4 \to 5 \to 4 \to 6 \to 4 \to y$ or the second time node 4 appears giving $x \to 2 \to 4 \to 6 \to 4 \to 5 \to 4 \to y$. The addition of two-step excursions can be iterated to generate longer and longer trips within each class. To do this, we take all of the trips generated at any given stage in the
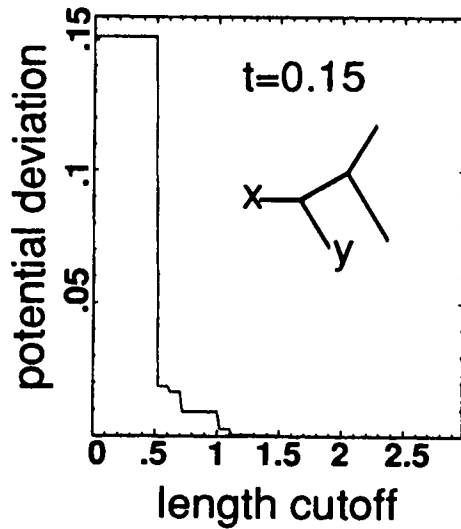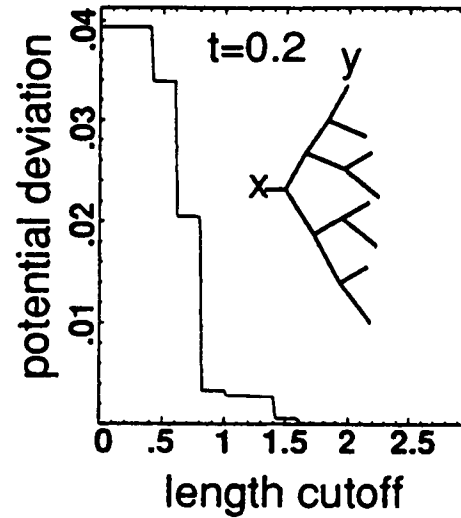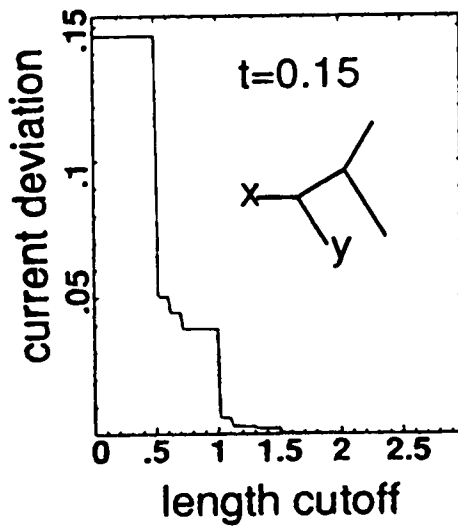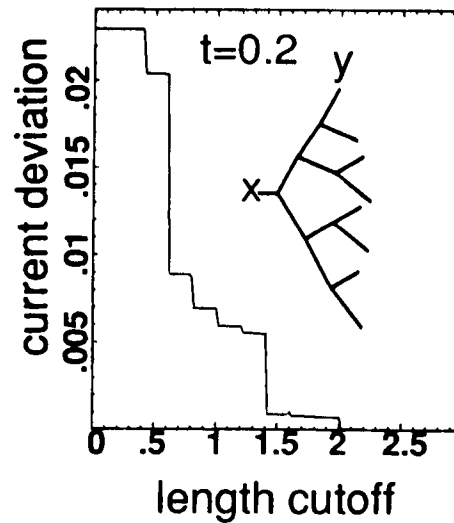
FIGURE 5 The potential and current deviations as defined in the text plotted as a function of the length cutoff. Panels *a* and *c* correspond to the tree of Fig. 2 *a*, and panels *b* and *d* to Fig. 2 *b*, with the upper plots showing potential and the lower plots current deviations. The plotted line falls discontinuously as the length cutoff is increased because of the finite length of the excursions being added. Beyond a cutoff of ~ 2 the deviations are too small to be seen on the plot.

process and add to each of the nodes and terminals in their sequences all possible two-step excursions. This technique generates all of the trips, but, as we saw in the example above, it can generate the same trip twice. Such double counting is eliminated by comparing each new trip that is generated to existing trips using an efficient binary search algorithm, and throwing the trip away if it

already has been included in the sum. Trips are also eliminated if the total length of the added excursions is greater than the cutoff length. Trips are constructed for all four classes and we keep generating trips until all the new trips being produced are longer than the maximum allowed length defined by the cutoff. While the trips are being generated, the lengths L_{trip} and coefficients A_{trip} are
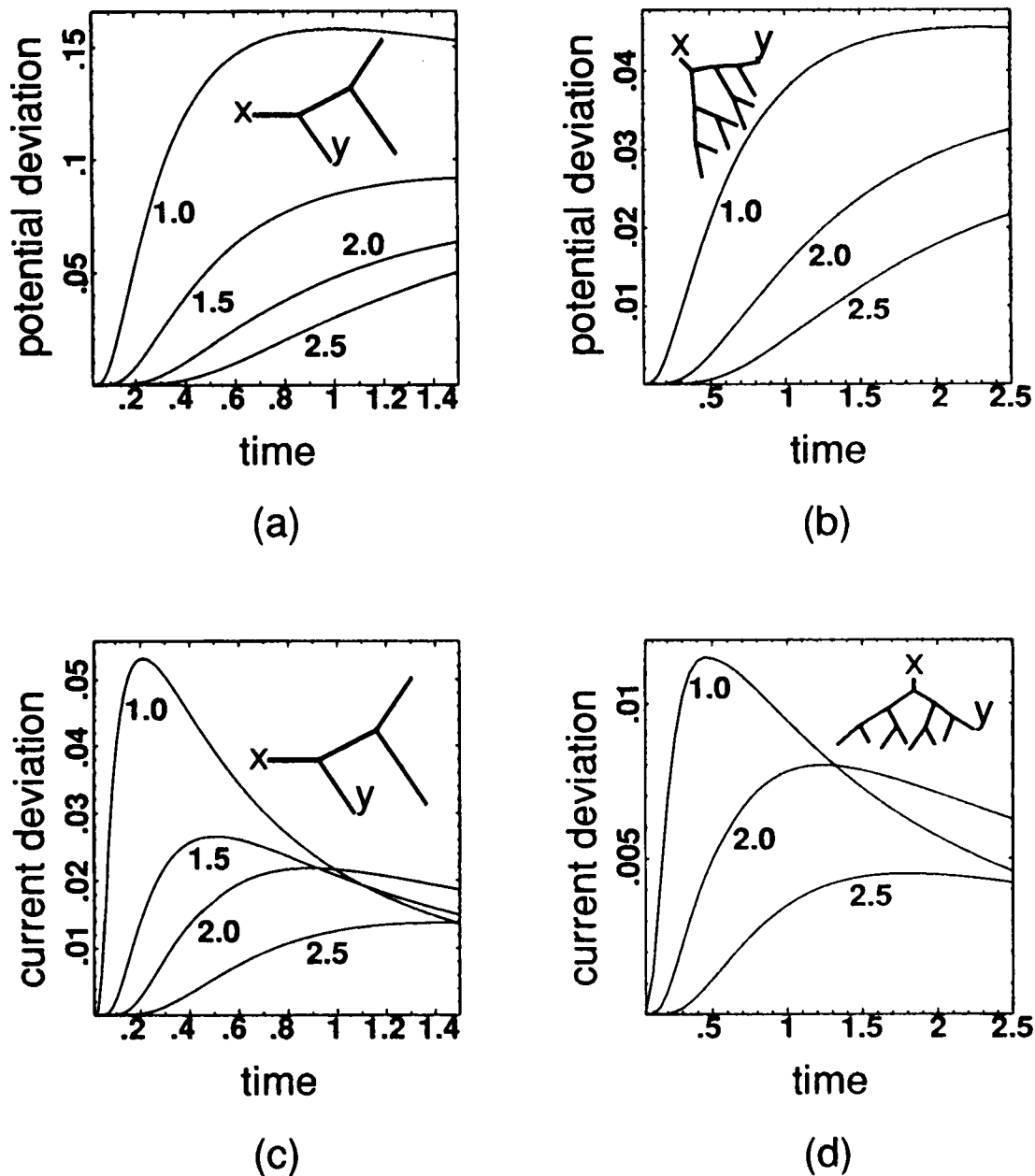
FIGURE 6 The potential and current deviations plotted as a function of time for the different length cutoff values indicated. Panels *a* and *c* are for the tree of Fig. 2 *a*, and panels *b*, and *d* for Fig. 2 *b*. Upper plots show potential and lower plots current deviations. The positions of *x* and *y* are as shown in the inserts.

computed and finally the Green's function is obtained from the sum of Eq. 2.1.

4. RESULTS

To illustrate the sum over trips calculation and to study its accuracy for different cutoff lengths, we consider the three sample trees shown in Fig. 2. All lengths and times in this and the following figures are measured in electrotonic units. Recall that the membrane potential $V(x, t)$ in response to a delta-function spike of current injected at the point y at time zero is given by $V(x, t) = G(x, y,$

$t) \exp(-t)$. Because of this, we plot $G(x, y, t) \exp(-t)$ rather than $G(x, y, t)$ in the figures. Typical results for the trees of Fig. 2 are shown in Fig. 3. In Fig. 3, the response to a delta-function input injected at the point marked y in the insert tree diagrams is plotted as a function of the point x where the potential is measured. The time t of the measurement, in units of RC, is indicated in the figures. The coordinate x measures the distance out from the base of the tree and the multiple lines indicate the potentials on different branches of the tree at equal electrotonic distances from the base. In Fig. 3 a, we show the potential for the tree of Fig. 2 a at three different

times to illustrate how the structure becomes more iso-potential as time progresses.

Fig. 4 allows us to examine the accuracy of the method for various cutoff lengths. For a cutoff of 3 to 4 electrotonic length units, the results have converged to the point where the errors in all three cases are smaller than the line width in the figures. This shows that the method converges for a reasonable cutoff length. What is extremely surprising is the accuracy of the sum over only the shortest trips in each of the four classes, corresponding to a cutoff of zero. In all the cases shown (and others we have studied), the sum of just four trips gives a remarkably good approximation to the exact answer. This is an extremely useful result, since the most accurate results shown here require the summation of tens of thousands of trips. If we want to estimate the potential quickly, we can sum the four terms generated by the shortest trip in each class. This is simple enough to be done by hand. The accuracy of this approximation tells us that the most important factors affecting the response of a tree are the length of the shortest path between the point where the potential is being measured and the point where current is being injected, the nature of the nodes located along this path, and properties of the nodes or terminals neighboring the points x and y. The accuracy of the four-trip sum depends on the presence of all four terms, leaving any of them out decreases the accuracy of the lowest-order approximation. Somehow the fact that these four trips contain information about the nodes or terminals on either side of both the measuring and the injection sites makes the four-term approximation considerably more accurate than we would have expected.

Fig. 4 also shows that the lowest order approximation with zero cutoff length converges to the exact answer at short times. In fact, the sum over just one trip, the shortest trip of all, can be used if t is small enough. The accuracy of the truncated sum at short times makes the method especially useful for determining short-time responses. Although the impact of the exponential suppression factor in Eq. 2.2 is less dramatic for larger t, the method is still useful in the long-time limit. Since the potential decreases like $\exp(-t)$, the response gets very small at large times and errors in its computation have little effect.

The sum over trips of Eq. 2.1 will satisfy the cable Eq. 1.1 no matter how few or how many terms are retained. Therefore the issue regarding the accuracy of the method is not whether the truncated sum satisfies the cable equation, but whether it satisfies the boundary conditions. These specify that at each node the Green's function measured along every radiating segment must converge to the same answer. Let $G_{seg}(x_{node})$ be the value of the Green's function evaluated on segment seg in the limit when x approaches the position of the node, x_{node}. Continuity of the potential requires that,

$$G_{seg}(x_{node}) = G_{seg'}(x_{node}) \qquad (4.1)$$

where seg and seg' label any two segments radiating from the node. To check how well this condition is satisfied for a truncated sum over trips, we define a potential deviation as follows. First we compute an average Green's function at each node,

$$\bar{G}(x_{node}) = \frac{1}{M} \sum_{seg \text{ on node}} G_{seg}(x_{node}) \qquad (4.2)$$

where M is the number of segments radiating from the node and the sum is over all M of these segments. The potential deviation for a tree, ΔV, is then defined by summing the squares of the differences of the Green's function for all pairs of segments radiating from a node, dividing by the average Green's function for that node and then averaging this over all nodes of the tree,

$$\Delta V = \left\langle \left(\sum_{seg > seg'} (G_{seg}(x_{node}) - G_{seg'}(x_{node}))^2 \right)^{1/2} \right.$$
$$\left. \times (\bar{G}(x_{node}))^{-1} \right\rangle \qquad (4.3)$$

where the angle brackets indicate the average over all the nodes of the tree.

A second set of boundary conditions requires that the current be conserved at every node and vanish at every terminal. The longitudinal current is proportional to the x derivative of the Green's function times the three-halves power of the segment radius. We will define $G'_{seg}(x_{node})$ to be the derivative of the Green's function taken along the direction of segment seg and evaluate at the node located at $x = x_{node}$. Similarly, $G'_{seg}(x_{term})$ is the derivative of the Green's function evaluated at a terminal of segment seg located at $x = x_{term}$. The current conservation boundary condition at a node is then

$$\sum_{seg \text{ on node}} \eta_{seg} a_{seg}^{3/2} G'_{seg}(x_{node}) = 0 \qquad (4.4)$$

where the factor η_{seg} is $+1$ for a parent branch at the node and -1 for the offspring branches. This corrects for whether the derivative corresponds to a current entering or leaving the node. The sealed-end boundary condition that we impose at terminals is

$$a_{seg}^{3/2} G'_{seg}(x_{term}) = 0 \qquad (4.5)$$

where seg labels the segment terminating at the given terminal. We define the current deviation for a tree by summing the absolute values of the quantities that should be zero according to the boundary conditions,

$$\Delta I = \left\langle \frac{1}{\bar{G}} \left| \sum_{seg \text{ on node}} \eta_{seg} a_{seg}^{3/2} G'_{seg}(x_{node}) \right| \right\rangle$$
$$+ \left\langle \left| \frac{a_{seg}^{3/2}}{G_{seg}(x_{term})} G'_{seg}(x_{term}) \right| \right\rangle \qquad (4.6)$$

where the first average $\langle \ \rangle$ is over all the nodes of the tree and the second is over all the terminals. $G_{seg}(x_{term})$ is the value of the Green's function at the terminal located at position $x = x_{term}$.

To check how well the boundary conditions are satisfied with a truncated sum, we show potential and current deviations for the trees of Fig. 2 a and 2 b in Figs. 5 and 6. Fig. 5 shows that at the times indicated all the deviations have been reduced to insignificant levels by the time the cutoff is greater than about 2. In Fig. 6, the deviations are small at short times because of the accuracy of the method in this limit. The deviations grow at larger times. The current deviations then decrease at still longer times because the tree becomes more isopotential. Note that the deviations decrease as the length cutoff is increased. The potential deviation increases in Fig. 6 as time increases and this may cause some concern as to the reliability of the method. However, it should be noted that the potential V will go to zero exponentially at large times due to the exponential factor in Eq. 1.2. The increase of the potential deviation is caused by the vanishing of the potential at large times. At large times, the absolute error of the truncated sum goes to zero but the percentage error grows as the potential decreases to zero.

6. DISCUSSION

The results we have shown indicate that the sum over trips is a useful technique for solving dendritic cable problems. Trips can be generated and summed by an efficient computer algorithm which, for reasonable cutoff lengths, gives accurate results. Even the lowest order approximation, consisting of just four trips, provides a fairly good estimate of the exact Green's function. The primary limitations of the method are that it assumes linear cables with uniform membrane conductance per unit area and that it ignores synaptic conductance changes.

Because the approach we use here is especially useful for investigating the short-time behavior of a cable, it can be used to quickly understand some interesting results obtained recently using compartmental methods (25). In recent years, the input impedence measured for hippocampal pyramidal neurons has increased dramatically. Since a higher input impedence means a larger membrane resistance R and a longer cable length constant, these new results were taken to imply that cable properties would play a reduced role for these cells. However, in the modeling studies of (25) it was found that significant deviations from isopotential behavior remained shortly after synaptic input activation even when the higher membrane resistance values were used. This result can be understood quite easily by using the sum over trips at short times.

Individual terms in the sum over trips are proportional to the Gaussian Green's function

$$G_0(L_{trip}, t) = \left(\frac{1}{4\pi t}\right)^{1/2} \exp\left[-\frac{L_{trip}^2}{4t}\right] \qquad (5.1)$$

where L_{trip} is the length of a given trip in units of the electronic length constants along the tree and t is mea-

sured in units of the membrane time constant. Recall that the membrane time constant is RC and the cable length constant for a segment of radius a is $(Ra/2r)^{1/2}$ where R is the membrane resistance. Because these units are being used, t is proportional to R^{-1} and L_{trip} is proportional to $R^{-1/2}$. As $t \to 0$, both the exponential in the above equation and the square root factor are singular, and at short times they determine the behavior of the potential. The Gaussian exponential, being the most singular element, is by far the most important term. The combination, $L_{trip}^2/4t$ appearing in the exponential is independent of R because L_{trip}^2 varies like R^{-1} as does t. As a result, the leading behavior of the potential at short times does not depend on the value of the membrane resistance. The square root factor introduces only a weak logarithmic dependence on R. Thus, we can understand the results reported for hippocampal neurons in (25) directly from the sum over trips formalism.

The algorithm we have used is quite efficient for trees that have segments with approximately equal lengths. However, if some segments are significantly shorter than others, it loses efficiency. This is because our algorithm generates trips in an essentially random order and then checks to see if they exceed the cutoff length. For trees with some short segments, it would clearly be advantageous to include some information to indicate that excursions across the short segments are more likely to yield trips shorter than the cutoff length than excursions traversing longer segments. This would not be difficult to do, and for specific applications would result in a significant increase in speed.

A dramatic increase in the efficiency of the program would be achieved if the algorithm could be modified so that it did not generate the same trip more than once. We have not explored this approach, but it should be possible to introduce rules that prevent the algorithm from duplicating the same trip, at least in many if not all cases. Alternately, it may be possible to compute the number of times that a particular trip is generated. Then, the contribution of this trip to the sum can be divided by this factor. This would eliminate the need for comparing trips to detect duplicates.

REFERENCES

1. Rall, W. 1977. Core conductor theory and cable properties of neurons. *In* Handbook of Physiology. Vol. 1. E. R. Kandel, editor. Am. Physiol. Soc., Bethesda, MD. 39–97.

2. Tuckwell, H. C. 1988. Introduction to Theoretical Neurobiology. Cambridge University Press, Cambridge. 2 Vols.

3. Jack, J. J. B., D. Noble, and R. W. Tsien. 1975. Electrical Current Flow in Excitable Cells. Oxford Univ. Press, Oxford. 415 pp.

4. Rinzel, J., and W. Rall. 1974. Branch input resistance and steady

attenuation for input to one branch of a dendritic neuron model. *Biophys. J.* 13:648–688.

5. Rinzel, J., and W. Rall. 1974. Voltage transients in neuronal dendritic trees. *Biophys. J.* 14:759–790.

6. Jack, J. J. B., and S. J. Redman. 1971. The propagation of transient potentials in some linear cable structures. *J. Physiol.* 215:283–320.

7. Wilson, C. J. 1984. Passive properties of dendritic spines and spiny neurons. *J. Neurosci.* 4:281–297.

8. Rall, W. 1962. Theory of physiological properties of dendrites. *Ann. NY Acad. Sci.* 96:1071–1092.

9. Butz, E. G., and J. D. Cowan. 1974. Transient potentials in dendritic systems of arbitrary geometry. *Biophys. J.* 14:661–689.

10. Koch, C., and T. Poggio. 1985. A simple algorithm for solving the cable equation in dendritic trees of arbitrary geometry. *J. Neurosci. Methods.* 12:303–315.

11. Holmes, W. R. 1986. A continuous cable method for determining the transient potential in passive trees of known geometry. *Biol. Cybern.* 55:115–124.

12. Horwitz, B. 1981. An analytic method for investigation transient potentials in branched neurons with branching dendritic trees. *Biophys. J.* 36:155–192.

13. Rall, W. 1964. Theoretical significance of dendritic trees for neuronal input–output relations. *In* Neural Theory and Modeling. R. Reiss, editor. Stanford University Press, Stanford, CA. 73–97.

14. Segev, I., J. W. Fleshmann, and R. E. Burke. 1989. Compartmental models of complex neurons. *In* Methods in Neuronal Modeling. C. Koch and I. Segev, editors. MIT Press, Cambridge, MA. 63–96.

15. Hines, M. 1984. Efficient computation of branched nerve equations. *J. Bio-Med. Comp.* 15:69–76.

16. Abbott, L. F., E. Farhi, and S. Gutmann. 1991. The path integral for dendritic trees. *Biol. Cybern.* 66:49–60.

17. Abbott, L. F. 1992. Simple diagrammatic rules for solving dendritic cable problems. *Physica A* 185:343–356.

18. Koch, C. 1984. Cable theory in neurons with active linearized membranes. *Biol. Cybern.* 50:15–33.

19. Koch, C., T. Poggio, and V. Torre. 1983. Nonlinear interactions in a dendritic tree: localization, timing and role in information processing. *Proc. Natl. Acad. Sci. USA.* 80:2799–2802.

20. Holmes, W. R., and C. D. Woody. 1988. The effectiveness of individual synaptic inputs with uniform and nonuniform patterns of background synaptic activity. *In* Cellular Mechanism of Conditioning and Behavioral Plasticity. C. D. Woody, D. Alkon, and J. McGaugh, editors. Plenum Press, NY. 345–362.

21. Holmes, W. R., and C. D. Woody. 1989. Effects of uniform and nonuniform synaptic activation-distributions on the cable properties of modeled cortical pyramidal neurons. *Brain Res.* 505:12–23.

22. Segev, I., and I. Parnas. 1989. Synaptic integration mechanisms: a theoretical and experimental investigation of temporal postsynaptic interaction between excitatory and inhibitory input. *Biophys. J.* 41:41–50.

23. Abbott, L. F. 1991. Realistic synaptic inputs for model neural networks. *Network: Computation in Neural Systems.* 2:245–258.

24. Cao, B. J. 1992. New method for solving dendritic cable equations. Ph.D. thesis. Brandeis University, Waltham, MA. 243 pp.

25. Brown, T. H., A. M. Zador, Z. F. Mainen, and B. J. Claiborne. 1991. Hebian computations in hippocampal dendrites and spines. *In* Single Neuron Computation. T. McKenna, J. Davis, and S. F. Zornetzer, editors. Academic Press, San Diego, CA. 81–116.